The Magnetic Ground State of Atacamite $Cu_2Cl(OH)_3$: The Crucial Role of Frustrated Zigzag Chains Revealed by Inelastic Neutron Scattering

J. L. Allen,[1,*] L. Stödter,[2,3] R. A. Mole,[4] S. Süllow,[2] O. Janson,[5] S. Nishimoto,[5,6] R. A. Lewis,[1] and K. C. Rule[4,1,†]

[1] *Institute for Superconducting and Electronic Materials and School of Physics, University of Wollongong, NSW 2522, Australia*

[2] *Institut für Physik der Kondensierten Materie, Technische Universität Braunschweig, D-38106 Braunschweig, Germany*

[3] *Jülich Centre for Neutron Science (JCNS) at Heinz Maier-Leibnitz Zentrum (MLZ), Forschungszentrum Jülich GmbH, 85748 Garching, Germany*

[4] *Australian Centre for Neutron Scattering, Australian Nuclear Science and Technology Organisation, Lucas Heights, NSW 2234, Australia*

[5] *Institute for Theoretical Solid State Physics, Leibniz Institute for Solid State and Materials Research Dresden, 01069 Dresden, Germany*

[6] *Department of Physics, Technical University Dresden, 01069 Dresden, Germany*

(Dated: March 18, 2026)

We report inelastic neutron scattering (INS) measurements on the magnetically frustrated $S = \frac{1}{2}$ sawtooth-chain compound atacamite $Cu_2Cl(OH)_3$ featuring inequivalent Cu(1) and Cu(2) sites. Transverse to the sawtooth chains, INS reveals two dispersive spin-wave modes and a gap of at least 0.75 meV. This behavior is rationalized within a zigzag-chain model of Cu(2) spins in an effective magnetic field of Cu(1) spins. The model is compatible with first-principles calculations and accounts for INS dispersions within linear spin-wave theory calculations. Our results reveal a unique case of an effective separation of energy scales between two differently oriented one-dimensional chains, with the zigzag-chain model being essential to fully characterize atacamite's low-energy magnetism.

I. INTRODUCTION

Frustrated spin systems offer the distinct potential to host novel exotic magnetic phases [1–4] and have become a platform through which to explore fundamental magnetism. The exotic phases emerge from specific magnetic interaction models. For instance, the corner-sharing tetrahedra of pyrochlore lattices can produce spin-ice states [3, 5, 6], and the kagome lattice is expected to host a quantum spin-liquid state [2]. Identifying experimental systems that realize these models allows for rigorous testing of theoretical predictions under real-world conditions.

Herbertsmithite ($ZnCu_3(OH)_6Cl_2$) [7] is one of the leading candidates for an experimental realization of a quantum spin-liquid material with its geometrically perfect spin-$\frac{1}{2}$ kagome lattice. It sits within the broader atacamite family of minerals [8], with the general formula $Zn_xCu_{4-x}(OH)_6Cl_2$ [9] encompassing polymorphs with various ratios of Zn-Cu substitution.

Atacamite ($Cu_2Cl(OH)_3$) refers to the orthorhombic polymorph of this mineral family, with full Cu^{2+} occupation. The spin-$\frac{1}{2}$ Cu^{2+} sites class atacamite as a quantum-magnetic system, and experiments have characterized its geometric frustration effects [10]. Furthermore, atacamite exhibits a complex magnetic phase diagram, including an antiferromagnetic ground state at T_N = 8.9 K [11] (with a magnetic propagation vector of $q = [\frac{1}{2}, 0, \frac{1}{2}]$ [12] and with suppressed magnetic moments of 0.34 μ_B and 0.59 μ_B for Cu(1) and Cu(2) sites, respectively) and a sequence of metamagnetic transitions up to 30 T, including a plateau-like behavior of the bulk magnetization above 31.5 T ($H \parallel b$ axis) [11]. However, the precise nature of these transitions and phases remained ambiguous.

Recently, a field-induced quantum critical point at 21.9(1) T ($H \parallel c$ axis) was identified at the low-temperature endpoint of the long-range ordered antiferromagnetic phase [13]. Further, the results from Ref. [13] underpinned the scenario of a dimensional reduction to an effectively one-dimensional behavior occurring at the quantum critical point as the residual 3D exchange couplings are overcome by the magnetic field energy. In this work, we explore the low-energy spin-wave excitations in zero applied field, allowing us to probe in detail the residual exchange couplings in atacamite responsible for the long-range magnetic order below T_N = 8.9 K and below the critical magnetic field.

Regarding the magnetic interactions driving the ground-state magnetism of atacmite, recent density functional theory (DFT) calculations indicate that the dominant exchange interactions form a weak 3D network of antiferromagnetic $S = \frac{1}{2}$ sawtooth chains [11]. The five strongest exchange pathways (J_1 = 0.11 meV, J_2 = −0.83 meV, J_3 = 8.79 meV, J_4 = 28.97 meV, and J_{11b} = 1.35 meV) are shown in Fig. 1, with the sawtooth chain running along the b direction. Interest has followed atacamite not only for its compositional similarities to Herbertsmithite, but also due to the unmatched opportunity it offers to *experimentally* investigate the complexities of a low-dimensional quantum spin system within the intensely-studied sawtooth chain model [14–21].

Although the sawtooth chain is the dominant coupling

* jlallen.correspondence@outlook.com
† kirrilyr@gmail.com

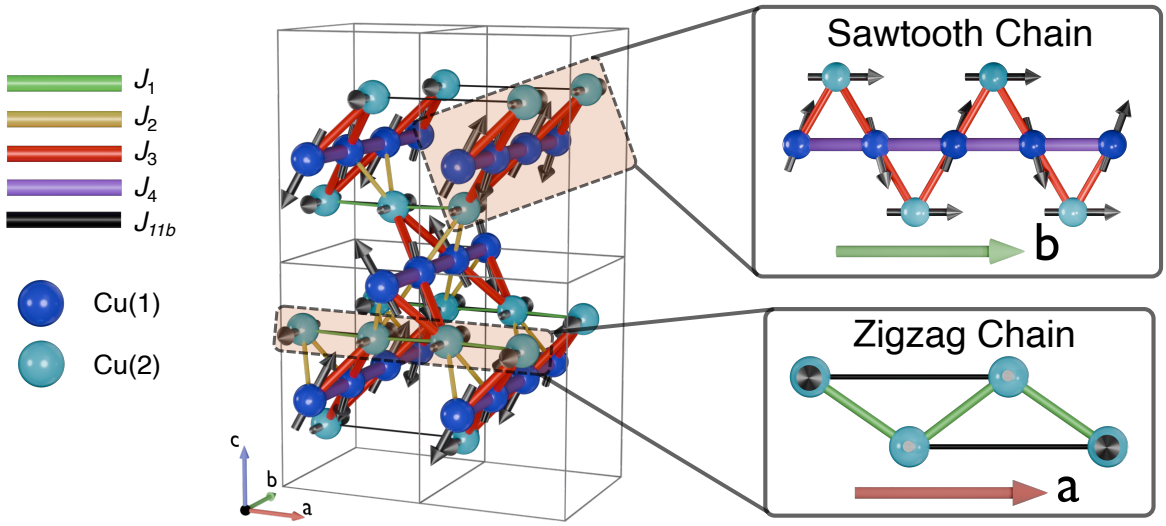

Figure 1. (Left) Magnetic structure derived from single-crystal neutron diffraction data [11], with exchange pathways from the 5 strongest exchange values according to the first-principles analysis in [11]. (Right) Expanded in-plane perspectives of the sawtooth-chain and zigzag-chain components in atacamite. The angles between the nearest-neighbor Cu(2) spins in the expanded zigzag chain have been greatly exaggerated for clarity.

motif in atacamite, DFT calculations also reveal a weaker perpendicular chain formed by competing nearest and next-nearest interactions [11]. This is the S=$\frac{1}{2}$ zigzag $J_1 - J_{11b}$ spin chain [22–25] (typically referred to as the $J_1 - J_2$ zigzag chain in the literature, and hereafter referred to as simply the 'zigzag chain' to avoid confusion with our exchange-label naming convention), with Hamiltonian

$$\mathcal{H} = \sum_{i=1}^{N} (J_1 \mathbf{S}_i \cdot \mathbf{S}_{i+1} + J_{11b} \mathbf{S}_i \cdot \mathbf{S}_{i+2}). \quad (1)$$

Here, J_1 and J_{11b} represent the nearest- and next-nearest-neighbor interactions, respectively, on a spin chain with an even number of N spin sites and spin-$\frac{1}{2}$ operators at spin site i.

The zigzag spin chain exhibits diverse magnetic phases dictated by the ratio of J_{11b}/J_1 [24, 26] owing to the complexity of the competing interactions. These include gapped and gapless spin states, spiral orders, and frustration-driven quantum phases such as spin-nematic states [24, 25] and spin-stripe phases. These states have also been revealed for material realizations of the zigzag chain [27–29].

In this investigation, we demonstrate that atacamite's zigzag chain plays a previously overlooked role in its magnetic behavior at low temperatures. We present the first investigation of atacamite's spin-wave excitation spectrum using inelastic neutron scattering (INS) within its ordered phase to directly probe its magnetic interactions. Similar approaches have been successfully employed to constrain and determine complex Hamiltonians in other $S = \frac{1}{2}$ zigzag-chain materials [30, 31]. We find that the zigzag chain is crucial for modeling atacamite, and, when combined with a mean-field treatment, an effective-model Hamiltonian for atacamite is produced that agrees with INS measurements in the low-energy regime. Furthermore, this agreement stands in contrast to the poor match obtained using the full DFT-derived model, whose dominant sawtooth chain is of a much higher energy scale than the zigzag chain. An effective separation of energy scales between the two chains is thus presented as an interesting characteristic of a material realization of a frustrated quantum magnet.

The compatibility between a magnetic model and INS measurements can only be justified within a robust theoretical framework. Linear spin-wave theory (LSWT) stands out as a straightforward, common [32], and reliable method for making quantitative comparisons between a magnetic Hamiltonian and INS experiments in long-range ordered spin systems.

LSWT and INS measurements are often used together to validate first-principles calculations and refine empirical magnetic models, including for frustrated (quantum) spin systems [5, 33–37].

The surprising success of LSWT in its application to quantum systems is rooted in the abundance of semiclassical behaviors [38], even in the $S = \frac{1}{2}$ limit [39] [30]. The LSWT calculations within this work were performed using the Sunny package [40] where the magnetic structure refined from neutron diffraction data [11] was chosen for the spin structure input.

II. EXPERIMENTAL METHODS

Single-crystal neutron scattering measurements of atacamite's spin-wave spectrum were performed at the

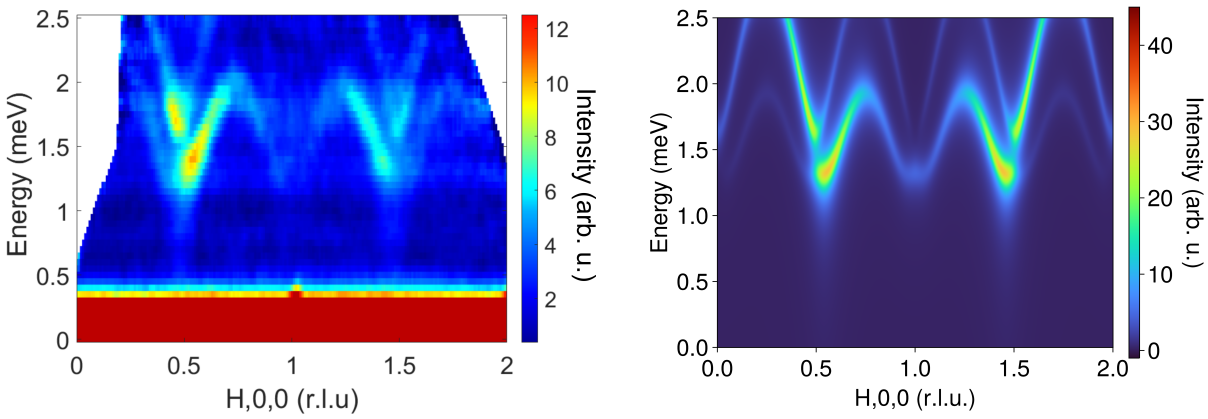

Figure 2. (a) Experimental INS data of (co-aligned) single-crystalline atacamite measured on Pelican at ANSTO at 1.5 K and at zero external field. Strong dispersion can be observed in the (H,0,0) direction with two separate nested modes. (b) LSWT calculations of the low-energy spin-wave modes in atacamite along (H,0,0) for a zigzag-chain model with an effective mean field $h = 0.26$ meV as defined in Eq. (2), using Sunny [40]. Note that normalized moment values have been used in this calculation, hence ignoring the effect of suppressed moments.

Australian Nuclear Science and Technology Organisation (ANSTO) on the Pelican [41] time-of-flight INS spectrometer with the sample rotated in the H0L plane. Pelican was configured with 4.69 Å neutrons and an approximate resolution of 0.135 meV at the elastic line.

The single-crystal INS data represents a four-dimensional dataset, comprising three spatial dimensions and one energy dimension. Although aligned in the H0L plane, the 0K0 direction could be measured out-of-plane up to $\pm 10°$ due the large detector height at Pelican of 1 m, resulting in ± 0.2 r.l.u. of measurable range in K.

Data were collected for the sample at 1.5 K, 6 K, and 20 K in a closed-cycle helium cryostat, and were measured across a sample rotation of 100° in 1° intervals. A vanadium sample was used to normalize the detector efficiencies and an empty cryostat scan was used for background subtraction.

Naturally-formed atacamite crystals were measured in this work. Atacamite crystallizes in an orthorhombic crystal structure with space group *Pnma* and with $a = 6.030(2)$ Å, $b = 6.865(2)$ Å, and $c = 9.120(2)$ Å[42] (see Section I in the supplemental material [43] for more details on the chemical unit cell).

Four single crystals of atacamite with a total mass of 1.8 g were co-aligned in the H0L plane using the high-intensity diffractometer Wombat [44]. Aluminium mounting methods were employed to avoid the effects of hydrogen from glue [45].

III. RESULTS

The INS data along the H-reciprocal-lattice direction, shown in Fig. 2a, is a 2D cut where neutron counts have been integrated within the interval [–2.5,2.5] along L, and [–0.2,0.2] along K. The data within the volume along L is relatively non-dispersive, and the intensity is distributed over a broadened energy range, as shown in Section VI of the supplemental material [43]. The measurements probe the low-energy region of atacamite's spin-wave excitations with an upper-energy threshold of 2.5 meV.

Along (H,0,0), two distinct, dispersive, energy-offset spin-wave modes are observed. A linear energy cut at H = 0.5 r.l.u. is shown in Fig. 3 and is taken with the same

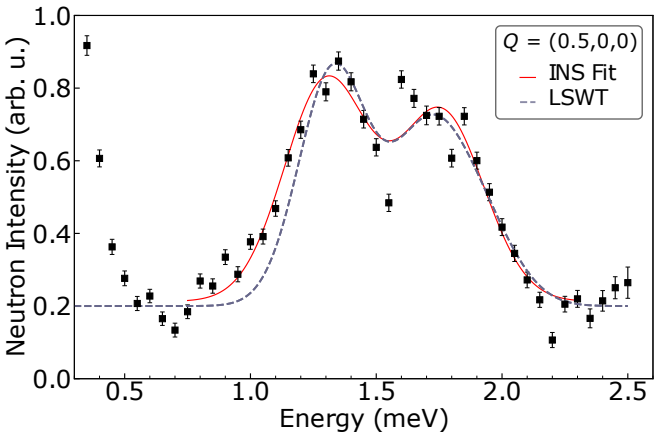

Figure 3. A constant-Q INS spectrum at (0.5,0,0). An integration width of Q = 0.04 r.l.u. has been used for the experimental data. A width of Q = 0.15 r.l.u. has been used for the LSWT-calculated data to mimic experimental broadening. The red line is a double Gaussian fit to the INS data and the dashed blue line is the Sunny LSWT calculation, equivalent to that in Fig. 2b. For the lower-energy INS mode, peak energy = (1.30 ± 0.03) meV and FWHM = (0.4 ± 0.1) meV. For the higher-energy INS mode, peak energy = (1.76 ± 0.03) meV and FWHM = (0.4 ± 0.1) meV.

integration widths in L and K as the H-dependent spectra in Fig. 2a, with an integration width of 0.04 r.l.u. in H. These data reveal two strong peaks in intensity – one at 1.7 meV and one at 1.3 meV. The lower-energy 1.3 meV peak is broad, and the neutron count doesn't reach the background level at the magnetic zone center until approximately 0.75 meV, as shown in Fig. 4 (see Fig. S10 [43] for more details on the gap quantification). Atacamite thus has an energy gap of at least 0.75 meV along the H00 direction, but, due to instrumental broadening, could be as high as the peak center of $\sim$ 1.3 meV, which would be compatible with the gap extracted from heat capacity measurements of approximately 1 meV [13].

LSWT calculations performed using the five strongest exchange interactions yielded by previous DFT results [11], which includes both the sawtooth and zigzag chains, fail to accurately reproduce all characteristics of these INS measurements. Specifically, spin-wave excitations appear at higher energies than are observed in the INS measurements, the asymmetry of the mode intensities do not match, and the lower-energy mode is not gapped (for further LSWT details for the full-DFT coupling network, see Figs. S5 and S6 [43]).

These shortcomings demonstrate that the full-DFT model does not adequately capture the magnetism governing atacamite's low-energy excitations within a semiclassical approach. The discrepancies in the full-DFT model may stem from the simplified treatment of quantum effects in LSWT, and could be alleviated in a fully quantum-mechanical treatment. Unfortunately, frustration and the three-dimensional nature of the full model make such treatment unfeasible. As an alternative, for a given energy scale, we can construct an effective model, which treats a subset of relevant exchanges exactly, while

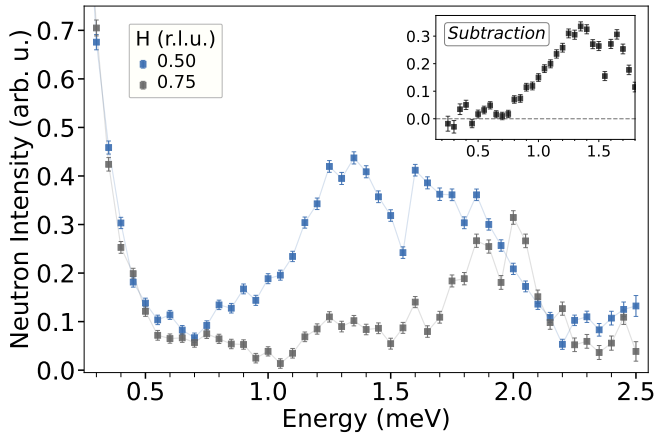

Figure 4. Constant-Q INS spectra at (0.50,0,0) and at (0.75,0,0), both with an integration width of Q = 0.04 r.l.u.. Neutron counts are within error of each other from below 0.75 meV, indicating that this is the minimum of the gap. The inset shows a subtraction of the constant-Q spectrum at (0.75,0,0) from the spectrum at (0.50,0,0). A fiducial line is drawn along zero counts to guide the eye.

other exchanges enter the model in a form of an effective field [22–25]. In atacamite, we achieve this by a mean-field treatment of the antiferromagnetic zigzag chain model along the a axis using the Hamiltonian

$$\mathcal{H} = \sum_{i=1}^{N} (J_1 \mathbf{S}_i \cdot \mathbf{S}_{i+1} + J_{11b} \mathbf{S}_i \cdot \mathbf{S}_{i+2} + \sqrt{2} h \sin[\frac{\pi}{4}(2i-1)] \mathbf{S}_i^y). \quad (2)$$

Here, J_1 is the nearest-neighbor interaction along a, J_{11b} is the next-nearest-neighbor interaction for the Cu(2) spins sites as defined in Fig. 1, and h is an effective staggered mean-field term which mimics the coupling to Cu(1) spins that are part of the sawtooth chains. The 4-fold periodicity of the staggered field has been constructed from observing the same periodicity in the ordering of the Cu(2) spin chain itself. This model is represented in Fig. 5.

The parameters of this model have been refined through a particle swarm algorithm comparing LSWT calculations to the INS data to find the global minimum. The refinement arrives at J_1 = 0.90 meV, J_{11b} = 1.91 meV, and h = 0.255 meV, giving a characteristic J_{11b}/J_1 ratio of 2.12. Classical LSWT calculations of the antiferromagnetic zigzag chain with ratios above $\sim$1 are qualitatively similar to exact diagonalization calculations (see Fig. S11 in the supplemental information [43]), suggesting quantum effects do not preclude semiclassical calculations from adequately characterizing the excitation spectrum in this system.

The refined LSWT scattering function calculation is shown in Fig. 2b. The result shows a remarkable qualitative match with experimental data along (H,0,0), namely the spin-wave amplitudes, the relative intensities of the dispersion, asymmetry in the dispersion intensities, the weakening intensity towards the magnetic zone boundary, the spin-wave frequencies, and, crucially, the spin-wave gap. A constant-Q cut of the calculated spin-wave spectra further confirms an excellent match with the experimental peak positions and gap size, as shown in Fig. 3.

The zigzag-chain model also provides critical insight into atacamite's gapped ground state. Theoretical considerations of the unmodified zigzag chain [22, 46] suggest that a J_{11b}/J_1 ratio of $\sim$0.5 would be required to produce a gap within the measured range of our INS data. Atacamite's much larger refined ratio of 2.12 would produce a gap in the order of only 0.1 meV [22]. This, and our observations that h directly and independently controls the gap size, suggest that the gap is instead primarily a result of interchain interactions modeled by the mean-field term. Consequently, interchain frustration, particularly via J_3 connecting the transverse chains, must be the dominant mechanism driving the observed gap. This is consistent with two observations. One – that the spin configurations of the Cu(1) and Cu(2) sublattices are near-perpendicular, a sign that the zigzag chain has adopted a compromised non-colinear configuration with respect to J_3 to minimize frustration. And two – the Cu(2) spins

have four-fold commensurate periodicity.

Without frustration, a zigzag chain is expected to adopt an incommensurate helical order which is nearly four-fold periodic [22]. The fact that the ground state is *exactly* four-fold commensurate implies that weak quantum fluctuations have selected this spin state through order-by-disorder from a frustration-induced classically degenerate set. This breaks symmetry, explaining the large observed gap [47].

While the LSWT-refined parameters provide a compelling and accurate model of the spin-wave excitations, they differ significantly from the initial DFT-calculated exchange values. The nominal DFT values were calculated using the generalized gradient approximation (GGA) method [48] with a Coulomb repulsion U-value of 8.24 eV [11]. These are $J_1 = 0.11$ meV and $J_{11b} = 1.35$ meV, with a J_{11b}/J_1 ratio of 12.27, which fail to provide agreement with INS measurements [43].

However, the U value has a drastic influence on the value and even the sign of J_1 [11], and hence also the J_{11b}/J_1 ratio, which plays the central role for the ground state. To inspect this difference closely, we performed new DFT calculations using the full-potential code FPLO version 22 [49]. We used the GGA supplemented with the Coulomb repulsion U which we varied in the range between 7 and 9 eV, and the Hund exchange of 1 eV. Further details of the calculations are provided in Section IV the supplemental information [43]. The GGA+U energies were mapped onto a classical Heisenberg model. In this way, we found that the LSWT-determined ratio J_{11b}/J_1 is reproduced by the interpolated values of $J_{11b} = 1.40$ meV and $J_1 = 0.66$ meV at $U = 7.75$ eV. The exchange-coupling values for initial DFT calculations from the literature, our new DFT calculations, and the fitting results for the zigzag chain are shown in Table I.

IV. DISCUSSION

Our results have revealed the critical nature of J_1 in modeling atacamite, and INS has allowed us to refine its highly U-sensitive value. These results, however, do not directly cast doubt on the validity of the previous DFT approach; the previous calculations correspond to the energy scale of the Curie-Weiss temperature [11], their dominant couplings agree with the Goodenough-Kanamori-Anderson rule [50–52] by association with atacamite's strongest Cu-O-Cu superexchange pathways, and they contain the very zigzag chain geometry used for our model.

Instead we make three key observations: Firstly, the zigzag chain plays an important role in atacamite's magnetism not previously explored. The necessity of the zigzag chain to reproduce the ordered-phase spin-wave dispersion at 1.5 K indicates that the zigzag-chain couplings are essential to the magnetic ordering behavior in atacamite. Atacamite's measured ground state behaves as a zigzag chain in a weak staggered field. It is therefore not enough to simply describe atacamite as a one-dimensional sawtooth chain system when discussing its long-range ordered phase.

Secondly, the energy scales between the zigzag and sawtooth chain are effectively separated by one order of magnitude, reflecting different roles in atacamite's spin dynamics. Although all *isotropic* couplings can be deduced simultaneously through DFT, low-energy spin-wave calculations performed with the full coupling scheme are unable to fully reproduce INS observations. Meanwhile, at temperatures far above $T_N = 8.9$ K, the Curie-Weiss temperature of ∼130 K derived from inverse susceptibility [12] aligns with the dominant energy scale of the sawtooth chain [11]. Additionally, magnetic order is suppressed near the energy scale of the zigzag chain [13], suggesting it governs atacamite's ordering dynamics.

This effective energy scale separation may be explained by frustration effects in atacamite. The refined mean-field term, $h = 0.26$ meV, is significantly smaller than the dominant interchain coupling predicted by DFT (∼ 9 meV), indicating that frustration suppresses the effective interchain coupling. Driven by J_3, this frustration not only inhibits long-range order by competing within the dominant sawtooth chain but also manifests itself through the order-by-disorder effects discussed earlier. As a result, atacamite's magnetic ground state is more sensitive to fluctuations, which both enhances the importance of subtle Hamiltonian terms, such as anisotropic interactions, and effectively separates the system into two distinct 1D coupling schemes. These same features also make it particularly challenging to construct a complete and precise model based on direct-exchange DFT pa-

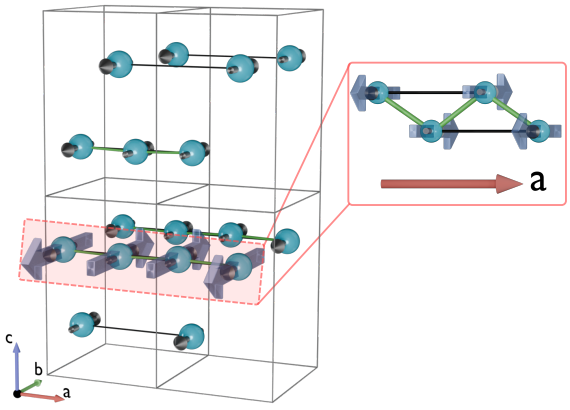

Figure 5. Atacamite's magnetic structure [11] and isotropic exchange interactions for the zigzag-chain model. To the right is the model shown for four Cu(2) atoms with exaggerated angles for clarity. Additionally, the staggered mean field components at each spin site for one spin chain are represented by transparent blue arrows pointing in the b direction, used to effectively model the residual coupling of the full 3D exchange network.

Table I. Exchange interactions for previous DFT calculations ($U = 8.24\,\text{eV}$) [11], our updated DFT calculations ($U = 7.75\,\text{eV}$), and the proposed zigzag-chain model whose values come from fitting LSWT calculations to the experimental INS data. Dashes (–) represent non-applicable values. A positive J-value corresponds to an antiferromagnetic coupling. An effective staggered mean field along the b axis is represented by h. Note that the 'New DFT' calculations do not include J_4 as part of the Hamiltonian (more details are in the supplemental [43]).

Exchange label	Previous DFT [11] (meV)	New DFT (meV)	Zigzag-Model LSWT Refinement (meV)
J_1	0.11	0.66	0.90
J_2	-0.83	-0.83	–
J_3	8.79	9.39	–
J_4	28.97	–	–
J_{11b}	1.35	1.40	1.91
h	–	–	0.26

rameters alone. Small inaccuracies in subtle interactions can become amplified in a fluctuation-influenced system, where semiclassical calculations may respond sensitively to such details.

Lastly, J_1 is extremely sensitive to U, which means a highly-precise determination of U is crucial for a model of atacamite. Through LSWT refinement against INS measurements, we have provided a significant and thorough refinement of the U value required to accurately describe atacamite in the low-temperature regime associated with long-range order.

V. CONCLUSIONS

LSWT calculations and INS measurements have revealed key insights into atacamite's magnetism in its long-range ordered phase. The mean-field-modified zigzag-chain model accurately reproduces the periodicity, intensity asymmetry, dispersion, and spin-wave gap observed in the INS data. The effective mean-field term h estimates the frustrated interchain interaction strength and provides insight into the spin-wave gap through an order-by-disorder mechanism.

In contrast, while prior DFT calculations for the dominant direct exchange couplings are consistent with high-temperature experimental results, they fail to account for the low-energy spin dynamics below the ordering temperature in a semiclassical LSWT treatment. This suggests that the DFT+U approach is unable to describe the magnetism across different energy scales with a single U value in this complex and frustrated magnetic system. Frustration also enhances quantum effects, suppressing weaker interactions such as interchain couplings. This has led to an effective energy scale separation between two distinct 1D-chain models. Nevertheless, by employing an effective model of a field-moderated zigzag chain, we successfully capture the essential features of the experimental dispersion relations and provide a reliable description of atacamite's low-energy magnetism. This way, we have uncovered the frustrated interchain exchange in atacamite leading to long-range magnetic order below its Néel temperature, and where the magnetic state is selected through order-by-disorder. In the light of the recent experimental results in high magnetic fields [13], it seems to be this frustrated interchain coupling network which is effectively broken up when the Cu(2) spins are fully field polarized in magnetic fields beyond the quantum critical point. Numerical results here supported the scenario of an (effective) dimensional reduction of the spin system upon which long-range magnetic order is suppressed.

Through establishing the exchange interactions outside the sawtooth chain in more detail, an avenue is now opened for building a clearer picture of the field-induced transitions which depend on the spin dynamics connected to these subtler interactions.

ACKNOWLEDGMENTS

This research used the Pelican time-of-flight spectrometer for proposal number P8226 at ACNS, a part of ANSTO, the Australian Nuclear Science and Technology Organisation. J. L. Allen would like to thank AINSE Limited for providing financial assistance (Award - PGRA) to enable this research. O.J. and S.N. were supported by the German Forschungsgemeinschaft (DFG, German Research Foundation) through SFB 1143 (Project ID 247310070). The authors acknowledge and thank A. U. B. Wolter from The Leibniz Institute for Solid State and Materials Research for her extensive contributions to atacamite research, and for constructive discussions while preparing the manuscript. Finally, we thank Ulrike Nitzsche for technical assistance.

[1] A. Banerjee, J. Yan, J. Knolle, C. A. Bridges, M. B. Stone, M. D. Lumsden, D. G. Mandrus, D. A. Tennant, R. Moessner, and S. E. Nagler, Neutron scattering in the

proximate quantum spin liquid α-$RuCl_3$, Science **356**, 1055 (2017).
[2] L. Balents, Spin liquids in frustrated magnets, Nature **464**, 199 (2010).
[3] S. T. Bramwell and M. J. P. Gingras, Spin ice state in frustrated magnetic pyrochlore materials, Science **294**, 1495 (2001).
[4] K. Binder and A. P. Young, Spin glasses: Experimental facts, theoretical concepts, and open questions, Reviews of Modern Physics **58**, 801 (1986).
[5] M. J. Harris, S. T. Bramwell, D. F. McMorrow, T. Zeiske, and K. W. Godfrey, Geometrical frustration in the ferromagnetic pyrochlore $Ho_2Ti_2O_7$, Physical Review Letters **79**, 2554 (1997).
[6] A. P. Ramirez, A. Hayashi, R. J. Cava, R. Siddharthan, and B. S. Shastry, Zero-point entropy in 'spin ice', Nature **399**, 333 (1999).
[7] M. R. Norman, Colloquium: Herbertsmithite and the search for the quantum spin liquid, Reviews of Modern Physics **88**, 041002 (2016).
[8] T. Malcherek, M. D. Welch, and P. A. Williams, The atacamite family of minerals – a testbed for quantum spin liquids, Acta Crystallographica Section B **74**, 519 (2018).
[9] P. Puphal, K. M. Zoch, J. Désor, M. Bolte, and C. Krellner, Kagome quantum spin systems in the atacamite family, Physical Review Materials **2**, 063402 (2018).
[10] X. G. Zheng, T. Mori, K. Nishiyama, W. Higemoto, H. Yamada, K. Nishikubo, and C. N. Xu, Antiferromagnetic transitions in polymorphous minerals of the natural cuprates atacamite and botallackite $Cu_2Cl(OH)_3$, Physical Review B **71**, 174404 (2005).
[11] L. Heinze, H. O. Jeschke, I. I. Mazin, A. Metavitsiadis, M. Reehuis, R. Feyerherm, J. U. Hoffmann, M. Bartkowiak, O. Prokhnenko, A. U. B. Wolter, X. Ding, V. S. Zapf, C. Corvalán Moya, F. Weickert, M. Jaime, K. C. Rule, D. Menzel, R. Valentí, W. Brenig, and S. Süllow, Magnetization Process of Atacamite: A Case of Weakly Coupled S=1/2 Sawtooth Chains, Physical Review Letters **126**, 207201 (2021).
[12] L. Heinze, R. Beltran-Rodriguez, G. Bastien, A. U. B. Wolter, M. Reehuis, J. U. Hoffmann, K. C. Rule, and S. Süllow, The magnetic properties of single-crystalline atacamite, $Cu_2Cl(OH)_3$, Physica B: Condensed Matter **536**, 377 (2018).
[13] L. Heinze, T. Kotte, R. Rausch, A. Demuer, S. Luther, R. Feyerherm, E. L. Q. N. Ammerlaan, U. Zeitler, D. I. Gorbunov, M. Uhlarz, K. C. Rule, A. U. B. Wolter, H. Kühne, J. Wosnitza, C. Karrasch, and S. Süllow, Atacamite $Cu_2Cl(OH)_3$ in High Magnetic Fields: Quantum Criticality and Dimensional Reduction of a Sawtooth-Chain Compound, Physical Review Letters **134**, 216701 (2025).
[14] T. Hamada, J. Kane, S. Nakagawa, and Y. Natsume, Exact solution of ground state for uniformly distributed rvb in one-dimensional spin-1/2 heisenberg systems with frustration, Journal of the Physical Society of Japan **57**, 1891 (1988).
[15] K. Kubo, Excited states and the thermodynamics of a fully frustrated quantum spin chain, Physical Review B **48**, 10552 (1993).
[16] S. Blundell and M. Núñez-Regueiro, Quantum topological excitations: from the sawtooth lattice to the heisenberg chain, The European Physical Journal B **31**, 453–456 (2003).
[17] K. Hida, Exotic ground state phases of s=1/2 heisenberg Δ-chain with ferromagnetic main chain, Journal of the Physical Society of Japan **77**, 044707 (2008).
[18] M. E. Zhitomirsky and H. Tsunetsugu, Exact low-temperature behavior of a kagomé antiferromagnet at high fields, Physical Review B **70**, 100403(R) (2004).
[19] A. Metavitsiadis, C. Psaroudaki, and W. Brenig, Enhancement of magnetization plateaus in low-dimensional spin systems, Physical Review B **101**, 235143 (2020).
[20] D. V. Dmitriev and V. Y. Krivnov, Delta chain with anisotropic ferromagnetic and antiferromagnetic interactions, Physical Review B **92**, 184422 (2015).
[21] D. V. Dmitriev and V. Y. Krivnov, Heisenberg–ising delta-chain with bond alternation, Journal of Physics: Condensed Matter **30**, 385803 (2018).
[22] S. R. White and I. Affleck, Dimerization and incommensurate spiral spin correlations in the zigzag spin chain: Analogies to the kondo lattice, Phys. Rev. B **54**, 9862 (1996).
[23] A. A. Aligia, C. D. Batista, and F. H. L. Eßler, Numerical method for detecting incommensurate correlations in the heisenberg zigzag ladder, Phys. Rev. B **62**, 3259 (2000).
[24] R. Bursill, G. A. Gehring, D. J. J. Farnell, J. B. Parkinson, T. Xiang, and C. Zeng, Numerical and approximate analytical results for the frustrated spin-1/2 quantum spin chain, Journal of Physics: Condensed Matter **7**, 8605 (1995).
[25] M. Kumar, A. Parvej, and Z. G. Soos, Level crossing, spin structure factor and quantum phases of the frustrated spin-1/2 chain with first and second neighbor exchange, Journal of Physics: Condensed Matter **27**, 316001 (2015).
[26] R. Valdés Aguilar, A. B. Sushkov, Y. J. Choi, S.-W. Cheong, and H. D. Drew, Spin-phonon coupling in frustrated magnet $CdCr_2O_4$, Physical Review B **77**, 092412 (2008).
[27] B. Willenberg, M. Schäpers, A. U. B. Wolter, S.-L. Drechsler, M. Reehuis, J.-U. Hoffmann, B. Büchner, A. J. Studer, K. C. Rule, B. Ouladdiaf, S. Süllow, and S. Nishimoto, Complex field-induced states in linarite $PbCuSO_4(OH)_2$ with a variety of high-order exotic SDW_p states, Physical Review Letters **116**, 047202 (2016).
[28] T. Vekua, A. Honecker, H.-J. Mikeska, and F. Heidrich-Meisner, Correlation functions and excitation spectrum of the frustrated ferromagnetic spin-1/2 chain in an external magnetic field, Physical Review B **76**, 174420 (2007).
[29] M. Pregelj, A. Zorko, O. Zaharko, H. Nojiri, H. Berger, L. Chapon, and D. Arčon, Spin-stripe phase in a frustrated zigzag spin-1/2 chain, Nature Communications **6**, 7255 (2015).
[30] M. Pregelj, O. Zaharko, U. Stuhr, A. Zorko, H. Berger, A. Prokofiev, and D. Arčon, Coexisting spinons and magnons in the frustrated zigzag spin-$\frac{1}{2}$ chain compound $\beta-TeVO_4$, Phys. Rev. B **98**, 094405 (2018).
[31] M. Hase, R. Tamura, K. Hukushima, S. Asai, T. Masuda, S. Itoh, and A. Dönni, Inelastic neutron scattering studies on the eight-spin zigzag-chain compound $KCu_4P_3O_{12}$: Confirmation of the validity of a data-driven technique based on machine learning, Phys. Rev. B **109**, 094434 (2024).
[32] R.-G. Zhu, Linear spin wave theory for the frustrated ferromagnetic spin chain in its incommensurate singlet

phase, Journal of Magnetism and Magnetic Materials **539**, 168323 (2021).
[33] T. Fennell, O. A. Petrenko, B. Fåk, S. T. Bramwell, M. Enjalran, T. Yavors'kii, M. J. P. Gingras, R. G. Melko, and G. Balakrishnan, Neutron scattering investigation of the spin ice state in $Dy_2Ti_2O_7$, Physical Review B **70**, 134408 (2004).
[34] J. T. Haraldsen, F. Ye, R. S. Fishman, J. A. Fernandez-Baca, Y. Yamaguchi, K. Kimura, and T. Kimura, Multiferroic phase of doped delafossite $CuFeO_2$ identified using inelastic neutron scattering, Physical Review B **82**, 020404 (2010).
[35] I. Mirebeau and S. Petit, Magnetic frustration probed by inelastic neutron scattering: Recent examples, Journal of Magnetism and Magnetic Materials **350**, 209 (2014).
[36] K. C. Rule, B. Willenberg, M. Schäpers, A. U. B. Wolter, B. Büchner, S.-L. Drechsler, G. Ehlers, D. A. Tennant, R. A. Mole, J. S. Gardner, S. Süllow, and S. Nishimoto, Dynamics of linarite: Observations of magnetic excitations, Physical Review B **95**, 024430 (2017).
[37] L. Heinze, M. D. Le, O. Janson, S. Nishimoto, A. U. B. Wolter, S. Süllow, and K. C. Rule, Low-energy spin excitations of the frustrated ferromagnetic J_1-J_2 chain material linarite $PbCuSO_4(OH)_2$ in applied magnetic fields parallel to the b axis, Phys. Rev. B **106**, 144409 (2022).
[38] J. Richter, J. Schulenburg, and A. Honecker, Quantum magnetism in two dimensions: From semi-classical Néel order to magnetic disorder, in *Quantum Magnetism*, edited by U. Schollwöck, J. Richter, D. J. J. Farnell, and R. F. Bishop (Springer, Berlin, Heidelberg, 2004) pp. 85–153.
[39] S. Ito, N. Kurita, H. Tanaka, S. Ohira-Kawamura, K. Nakajima, S. Itoh, K. Kuwahara, and K. Kakurai, Structure of the magnetic excitations in the spin-1/2 triangular-lattice Heisenberg antiferromagnet $Ba_3CoSb_2O_9$, Nature Communications **8**, 235 (2017).
[40] Sunny (v.0.7.2), https://github.com/SunnySuite/Sunny.jl.
[41] Yu, Dehong, Mole, Richard. A., and Kearley, Gordon J., Performance test on pelican - a multi-purpose time of flight cold neutron spectrometer, EPJ Web of Conferences **83**, 03019 (2015).
[42] J. B. Parise and B. G. Hyde, The structure of atacamite and its relationship to spinel, Acta Crystallographica Section C **42**, 1277 (1986).
[43] See Supplemental Material at [link], for details of the full INS dataset, and further theoretical details.
[44] A. J. Studer, M. E. Hagen, and T. J. Noakes, Wombat: The high-intensity powder diffractometer at the opal reactor, Physica B: Condensed Matter **385-386**, 1013 (2006).
[45] K. C. Rule, R. A. Mole, and D. Yu, Which glue to choose? A neutron scattering study of various adhesive materials and their effect on background scattering, Journal of Applied Crystallography **51**, 1766 (2018).
[46] A. Lavarélo and G. Roux, Spinon excitation spectra of the J1-J2 chain from analytical calculations in the dimer basis and exact diagonalization, The European Physical Journal B **87**, 229 (2014).
[47] C. L. Henley, Ordering due to disorder in a frustrated vector antiferromagnet, Physical Review Letters **62**, 2056 (1989).
[48] J. P. Perdew, K. Burke, and M. Ernzerhof, Generalized gradient approximation made simple, Phys. Rev. Lett. **77**, 3865 (1996).
[49] K. Koepernik and H. Eschrig, Full-potential nonorthogonal local-orbital minimum-basis band-structure scheme, Phys. Rev. B **59**, 1743 (1999).
[50] J. B. Goodenough, Theory of the role of covalence in the perovskite-type manganites [La, m(II)]MnO_3, Phys. Rev. **100**, 564 (1955).
[51] J. Kanamori, Superexchange interaction and symmetry properties of electron orbitals, Journal of Physics and Chemistry of Solids **10**, 87 (1959).
[52] X. Rocquefelte, K. Schwarz, and P. Blaha, Theoretical investigation of the magnetic exchange interactions in copper(II) oxides under chemical and physical pressures, Scientific Reports **2**, 759 (2012).